Optimization of a Multiphase Sensor for Detection of Phosphonates in Air

Chelsea N. Monty, Ilwhan Oh, and Richard I. Masel
Dept. of Chemical and Biomolecular Engineering, University of Illinois at Urbana-Champaign, Urbana, IL 61801

DOI 10.1002/aic.11946
Published online October 21, 2009 in Wiley InterScience (www.interscience.wiley.com)

The objective of this article is to report the modeling and optimization of a new MEMS-based phosphonate sensor that utilizes a porous membrane between a gas and a liquid stream to allow operation at low-liquid and high-gas flow rates. Previous work from our laboratory demonstrated that phosphonate molecules can be detected with such a device, but the sensitivity was insufficient for certain applications (e.g., detection of pesticides in foodstuffs). In this article, COMSOL simulations and design of experiments were used to optimize the device. We find that both the simulation and the experiment show that (i) the size of the pores in the membranes and (ii) the liquid channel height make the most difference to the sensor response. Also, by optimizing the geometry, the sensitivity of the device could be enhanced. The optimized device can detect 10^9 molecules with good signal to noise. © 2009 American Institute of Chemical Engineers *AIChE J*, 56: 241–247, 2010

Keywords: COMSOL simulation, microreactor, gas–liquid interface, nanoporous membrane

Introduction

According to recent reviews, there is a critical need for more sensitive and more selective portable sensors for toxic phosphonates.[1–4] Consequently, there is a need for improved sensor designs. In previous papers,[5,6] we presented a new sensor design that showed better sensitivity and selectivity than any previously reported portable sensor detection of phosphonates in air. Our sensor design is advantageous, because it uses a selective liquid chemistry to detect trace amounts of highly toxic chemicals in air. The sensor consists of a gas channel and a liquid channel separated by a porous membrane, as shown in Figure 1. Air containing the phosphonates flows through the gas channel at high velocity. The phosphonates diffuse out of the air and dissolve into the liquid, where they react via Scheme 1 to yield a cyanide ion that can be detected electrochemically.[7] The reaction is selective to alkalating phosphonates and few related compounds (e.g., isopropyl sulfonyl chloride, acetic anhydride[8]).

Correspondence concerning this article should be addressed to R. I. Masel at r-masel@uiuc.edu

We chose the two-chamber design because we wanted to use a high-vapor flow rate and a low-liquid flow rate. The high-vapor flow rate gives a fast response, whereas the low-liquid flow rate allows us to minimize the reagents used in the process. Most two-phase microfluidic designs show unstable interfaces under the conditions of interest here.[9–14] The use of the membrane allowed us to stabilize the interface, and thereby achieve lower detector noise and greater reproducibility.

Our previous papers,[5,6] demonstrated that the detection system worked and had better sensitivity and selectivity than any phosphonate detector reported previously. However, the response time and sensitivity of the sensor are still not at the desired levels for real-world phosphonate detection (e.g., detection of pesticide vapors in food). Calculations show that our initial sensor geometry is limited by the large resistances due to the mass transport of phosphonate molecules across the gas–liquid interface and into the liquid microchannel. Therefore, improvements in sensor geometry were possible.

The objective of the work reported in this article was to optimize the design by (1) using COMSOL simulations to optimize the geometry and understand which variables were

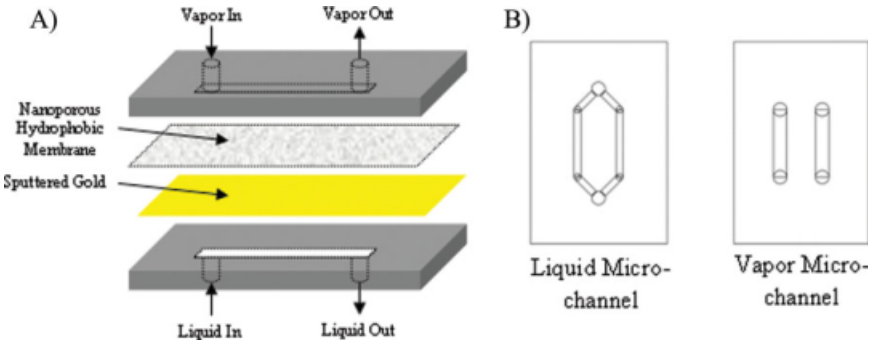

Figure 1. (A) Schematic of the dual microchannel/membrane system. Vapor flows through the top microchannel (0.25 mm wide by 0.1 mm deep) and is separated from the liquid microchannel (0.25 mm wide by 0.1 mm deep) by a nanoporous membrane (0.006 mm thick) with 40 nm of sputtered gold on the membrane surface closest to the liquid microchannel. (B) Double microchannel design.

[Color figure can be viewed in the online issue, which is available at www.interscience.wiley.com.]

important to the response, (2) verify the model experimentally, and (3) use the results to improve the sensitivity of the device.

Experimental Methods

Fabrication of the microchannel sensor

The assembly of the microchannel sensor involves three steps: (1) fabrication of microchannels, (2) deposition of the electrode onto a nanoporous membrane, and (3) assembly of the gas and liquid microchannels and the nanoporous membrane. The microchannels were machined into a small polycarbonate block. To make the membrane coated with an electrode, track-etch polycarbonate membranes of various pore sizes (thickness 6 μm; SPI) are sputtered with a 40-nm thick layer of gold on the side of the liquid microchannel. The track-etch membranes are purchased from SPI without the PVP coating. The gas microchannel is made to overlap the liquid microchannel. The membrane is sandwiched between the two polycarbonate microchannels and the assembly is bonded using epoxy. A schematic of the final assembly is found in Figure 1.

Preparation of chemicals

The oxime solution is 10 mM 1-phenyl-1,2,3,-butanetrione 2-oxime (PBO, Aldrich) in a borate buffer (pH = 10). Because oxime degrades and loses reactivity over several days, fresh oxime solution is prepared for every experiment. The chemical vapors, which are passed along the gas microchannel, are sampled with a syringe from pure liquid chemicals in a bubbler and diluted with ambient air to the desired vapor concentration.

Testing of the microchannel sensor

The testing set-up of the oxime sensor is the same as that of our previous work by Oh et al.[7] A dual microchannel design is used with a reference and active liquid microchannel (Figure 1B). The oxime solution is passed along the liquid microchannels using a manually operated syringe. During electrochemical measurements, the liquid in the microchannels remains static. After each measurement, fresh oxime solution is passed through the liquid microchannels to remove reaction products present in the sensor. The vapor sample is introduced into the active gas microchannel using a syringe pump containing the diluted chemical sample at the flow rate of 1 mL/min. The open-circuit potential between the active membrane electrode and the reference membrane electrode is measured as the output signal from the microchannel sensor. By measuring the electrode potential of a gold electrode in diluted standard cyanide solution, the equation for the CN^- concentration determined to be the following:

$$E = 1255[CN^-]^{0.22}$$

where E is the open-circuit potential in millivolts. Open circuit potential was measured at various channel geometry, membrane pore size, and pore hydrophilicity.

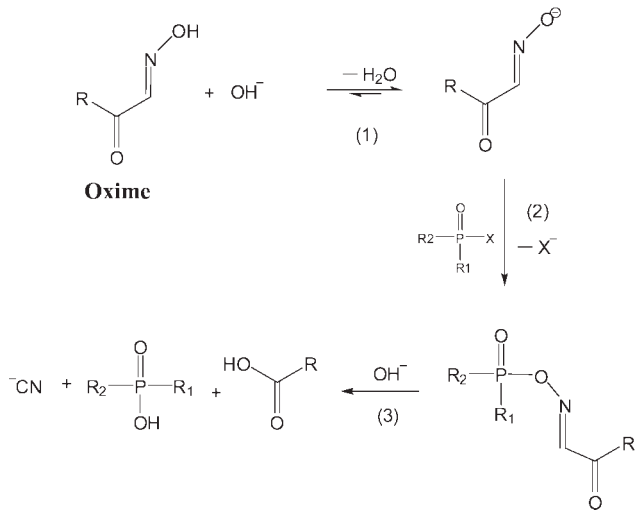

Scheme 1. The reaction between an oxime and organophosphorous compound to yield a cyanide that can be detected electrochemically.

Table 1. Physical Constants for COMSOL Simulation of Multiphase Microreactor

Name	Expression	Description	Reference
K_H	0.55	Henry's Law Constant (atm cm^3 mol^{-1})	16
k	5.79×10^3	Approximate reaction constant (cm^3 $mole^{-1}$ min^{-1})	15
D_{gas}	0.01	Diffusivity of vapor-phase molecules (cm^2/s)	8
D_{liquid}	1×10^{-5}	Diffusivity of liquid-phase molecules (cm^2/s)	8
$C_{initial,oxime}$	1×10^{-5}	Initial concentration of oxime in solution (mol/cm^3)	5
$C_{phosphonate}$	4.5×10^{-12}	Concentration of phosphonate vapor (mol/cm^3)	5

Numerical Simulation Using COMSOL Multiphysics

A numerical simulation of cyanide concentration in the liquid microchannel and phosphonate concentration in the vapor microchannel was performed over a range of channel geometry and membrane pore size using COMSOL Multiphysics 3.3 and the Chemical Engineering Module. The model assumed that liquid was static and the air flowed parallel to the microchannels. We then solved the equations of motion in three different regimes: the liquid channel, the gas channel, and the porous membrane.

The constants used in the simulation can be found in Table 1. Air and liquid diffusion coefficients of $D_{gas} = 0.01$ cm^2/s and $D_{liquid} = 1 \times 10^{-5}$ cm^2/s were used.[8] The diffusivity of phosphonate vapor through a hydrophobic membrane, D_m, was estimated using a model for gas diffusion in porous media[17]:

$$D_m = D_{gas}\varepsilon^{\frac{4}{3}} \quad (1)$$

where ε is the porosity of the nanoporous membrane. The value of ε varies with respect to pore size by the following:

$$\varepsilon = \frac{n\left(\frac{\pi \cdot d^2}{4}\right)}{w \cdot l} \quad (2)$$

where n is the number of pores, d is pore diameter, w is channel width, and l is channel length.[17] When simulating transport through PVP-coated, hydrophilic pores, it is assumed that the pores are wicked with liquid.

Concentration of phosphonate vapor (4.5×10^{-5} mol/cm^3) and initial concentration of oxime solution (1×10^{-5} mol/cm^3) were taken from the experimental procedure. The reaction rate follows a second-order rate law with respect to oxime and phosphonate concentration and has a rate constant (k) of 5.79×10^3 cm^3 $mole^{-1}$ min^{-1}.[8]

Results and Discussion

Results from COMSOL simulation

Figure 2 shows simulation results of how the phosphonate concentration varies perpendicularly to the membrane at a point 0.125 cm from the leading edge of a 0.0075 cm deep, 0.25 cm long microchannel. The simulation assumed that the membrane was a 0.0006-cm thick with 50-nm hydrophobic pores, the liquid microchannel contains 10 mM oxime solution and 1 cm^3/min of gas containing 100 ppb of analyte flows in the vapor microchannel. Note that the analyte concentration is almost constant in the gas phase then decays exponentially into the liquid. These results suggest that most of the mass transfer resistance is in the liquid side of the membrane, since diffusivities are so much lower in the liquid phase than in the gas phase.

The simulation was then used to vary multiple geometric reactor parameters, to determine their effect on sensor response. Simulation results show that varying the width and length of the microchannels has no effect on the sensor response. Width is changed in our two-dimensional simulation by varying the superficial velocity. Changing parameters, such as channel depth and pore size, however, had a large effect on sensor response. It should be noted that changing the pore size and channel depth should have the largest effect on response.

Figure 3A shows simulations results for the effect of pore size in the nanoporous membrane on sensor response for a microchannel 0.25 mm wide, 0.1 mm deep, and 5 mm long with hydrophobic pores. In this simulation, the liquid microchannel contains 10 mM oxime solution and 1 cm^3/min of gas containing 100 ppb of analyte flows in the vapor microchannel and response is measured after 30 s. Note that as pore size increases from 10 to 100 nm, the sensor response increases in the form of cyanide ion concentration. Figure 3C shows that mass transport across the membrane increases proportionally with larger pores due to an increase in open

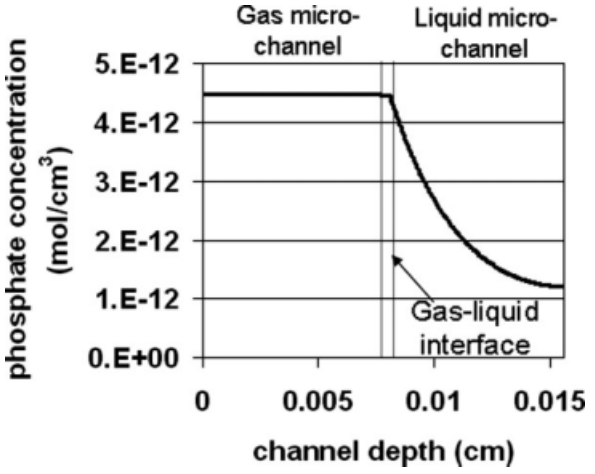

Figure 2. Simulation results for the phosphonate concentration profile along the depth of the microreactor.

The microchannels are 0.0075 cm deep and are separated by a 0.0006 cm thick membrane and the concentration profile is taken at a position halfway down the length of the microreactor (0.25 cm) after 90 s. The nanoporous membrane contains pores that are 50 nm in diameter and are considered hydrophobic. Phosphonate enters the microreactor at 4.5×10^{-12} mol/cm^3 and the gas–liquid interface is saturated with phosphonate vapor. Phosphonate enters the liquid microchannel and begins to react with oxime solution.

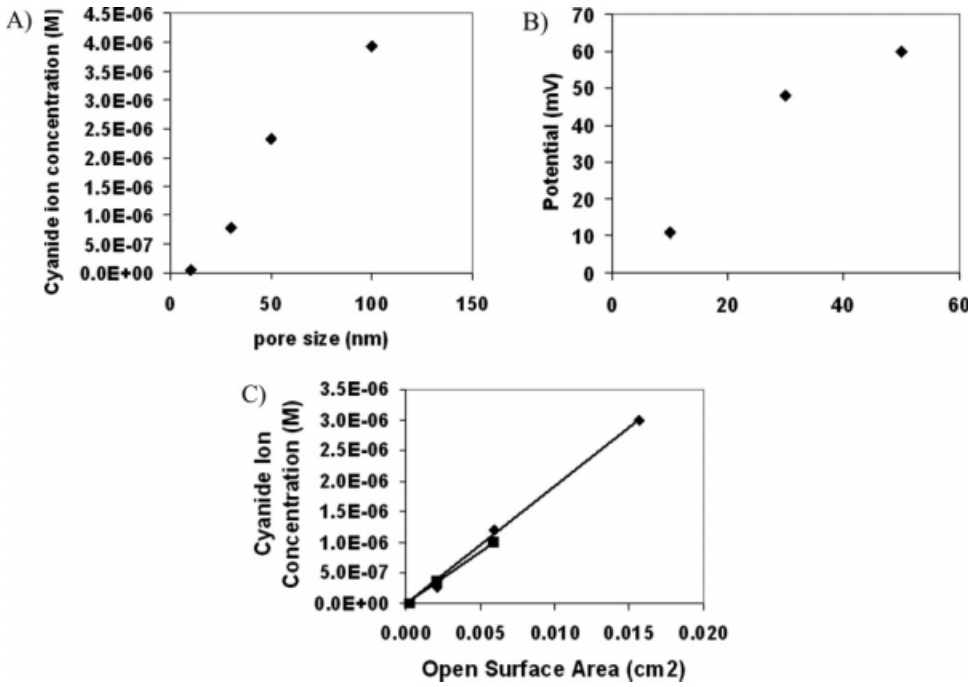

Figure 3. (A) Simulation results for the effect of pore size in the nanoporous membrane on sensor response.

Cyanide ion concentration reported is for a microchannel that is 0.25 mm wide × 0.1 mm deep × 5 mm long after a time of 30 s; the liquid microchannel contains 10 mM oxime solution with 100 ppb analyte gas at a flow rate of 1 cm^3/min in the vapor microchannel and the cyanide concentration is measure after 30 s. (B) Experimental results for the effect of pore size of the nanoporous membrane on sensor response; the liquid microchannel (0.25 mm wide × 0.10 mm deep × 5 mm long) contains 10 mM oxime solution in borate buffer (pH = 10) with 100 ppb analyte gas at a flow rate of 1 cm^3/min in the vapor microchannel; the potential is reported after 30 s. (C) Effect of open surface area on cyanide ion concentration. Calculated (black diamonds) and experimental results (black squares) are reported as cyanide ion concentration. Dimensions and experimental procedure are the same as those listed above.

surface area and therefore porosity of the nanoporous membrane. The larger open surface area increases the gas–liquid interface and allows more phosphonate molecules to cross into the liquid microchannel.

Figure 4 shows the effect of channel depth on sensor response from the COMSOL simulation for a microchannel 0.25 mm wide and 1 cm long with 50 nm hydrophobic pores. In this simulation, the liquid microchannel contains 10 mM oxime solution and 1 cm^3/min of gas containing 100 ppb of analyte flows in the vapor microchannel and response is measured after 30 s. Note that as the channel depth decreases from 0.2 mm to 0.05 mm, the sensor response increases in the form of increased cyanide concentration. The increase in response may be due to a build up of cyanide ions or phosphonate molecules near the gas–liquid interface caused by a smaller amount of liquid in reduced channel depths.

Experimental results with oxime microreactor

After study of the statistical analysis of the COMSOL simulation, a design of experiments was completed based on the simulated data. From the simulation results, it was noted that varying channel length and channel width did not have a large effect on sensor response while varying channel depth and pore size. Therefore, testing of the oxime microreactor focused on changing channel geometry and pore size to determine the effect of each on sensor response.

Figure 5 shows experimental results for the response of an oxime microreactor to phosphonate vapor for a microchannel 0.05 mm deep, 0.25 mm wide, and 5 mm long. In this experiment, the liquid microchannel contains 10 mM oxime solution and 1 cm^3/min of gas containing 100 ppb of analyte flows in the vapor microchannel after 15 s. Note that the sensor response occurs within seconds and the mass transport of phosphonate molecules across the nanoporous membrane and into the liquid microchannel is fast enough for the oxime microreactor to be a viable, rapid-response phosphonate sensor.

Figure 3B shows experimental results for the effect of the pore size in the nanoporous membrane on sensor response for a liquid microchannel 0.25 mm wide, 0.10 mm deep. In this experiment, the liquid microchannel contains 10 mM oxime solution and 1 cm^3/min of gas containing 100 ppb of analyte flows in the vapor microchannel and potential is recorded after 30 s. Note that as the pore size increases from 10 to 50 nm the response of the sensor also increases from 11 to 60 mV (Pore sizes above 50 nm could not be tested due to flooding of the oxime solution into the vapor microchannel). Figure 3C shows that mass transport across the membrane increases proportionally with larger pores due to

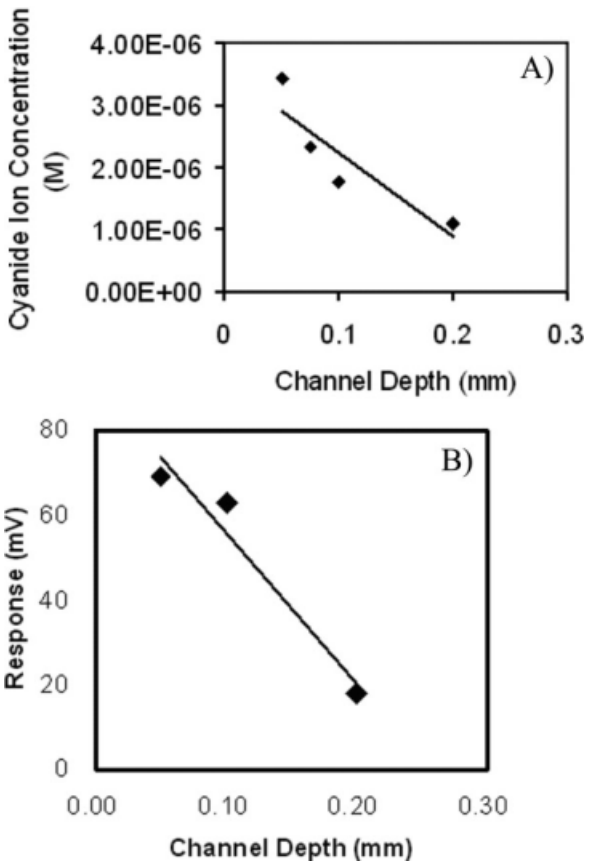

Figure 4. (A) Simulation results for the effect of channel depth on cyanide ion concentration.

The microchannels are 0.25 mm wide and 10 mm long with 50 nm pores in the nanoporous membrane. The liquid microchannel contains 10 mM oxime solution with 100 ppb analyte gas at a flow rate of 1 cm^3/min in the vapor microchannel and the cyanide concentration is measured after 30 s. (B) Experimental results for the effect of channel depth on sensor response.

The liquid microchannel is 5 mm long by 0.25 mm wide and the depth of the channel is varied (pore size = 50 nm). The liquid microchannel contains 10 mM oxime solution in borate buffer (pH = 10) with 100 ppb analyte gas at a flow rate of 1 cm^3/min in the vapor microchannel. The potential is reported after 30 s.

an increase in open surface area and therefore porosity of the nanoporous membrane. The larger open surface area increases the gas–liquid interface and allows more phosphonate molecules to cross into the liquid microchannel.

Figure 4B shows the experimental effect of channel depth on sensor response for a 5 mm long liquid microchannel with varying channel depth with 50 nm PVP-free membranes. In this experiment, the liquid microchannel contains 10 mM oxime solution and 1 cm^3/min of gas containing 100 ppb of analyte flows in the vapor microchannel and potential is recorded after 30 s. Note that as the channel depth decreases from 0.2 mm to 0.05 mm the sensor response increases. These results may be due to an increased build-up of cyanide ions or phosphonate molecules at the electrode surface for smaller channel depths.

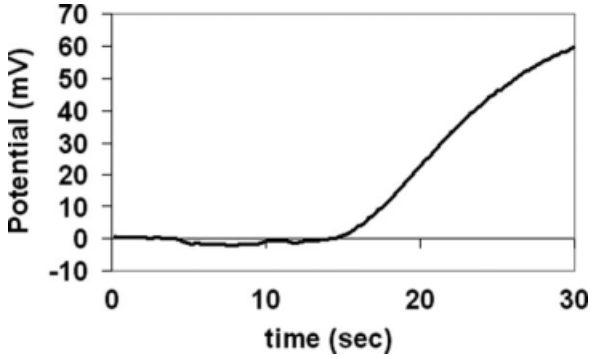

Figure 5. Experimental sensor response vs. time for the oxime microreactor after exposure to phosphonate vapor.

The liquid microchannel (0.05 mm × 0.25 mm × 5 mm) contains 10 mM oxime solution in borate buffer (pH = 10). The phosphonate analyte (100 ppb) is introduced after 15 s at a flow rate of 1 cm^3/min and the sensor shows a response almost instantly proving the oxime microreactor can be a viable rapid-response phosphonate sensor.

Figure 6 shows the experimental results for the effect of vapor residence time on sensor response for a liquid microchannel 0.25 mm wide, 0.10 mm deep, and 5 mm long. In this experiment, the liquid microchannel contains 10 mM oxime solution and 1 cm^3/min of gas containing 100 ppb of analyte flows in the vapor microchannel, and potential is recorded after 30 s. Note that the vapor residence time has very little effect on the sensor response with an average potential response of 73 mV.

Comparison of Experimental Data and Numerical Simulation

A comparison of the numerical simulation and experimental data is shown in Table 2. Note that in both experimental results and numerical simulations, varying the channel length, and channel width had little to no statistical affect

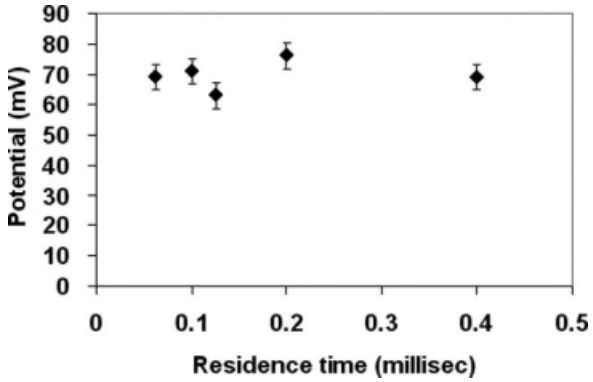

Figure 6. Experimental results for the effect of vapor residence time on sensor response.

The liquid microchannel contains 10 mM oxime solution in borate buffer (pH = 10) with 100 ppb phosphonate analyte gas at a flow rate of 1 cm^3/min in the vapor microchannel. The potential is reported after 30 s with an average potential response of 73 mV and a standard deviation of 8.5 mV.

Table 2. Comparison of Experimental Data to Simulation Results for Varying Geometric Reactor Parameters

Geometric Parameter	Range Studied	Slope Calculated from Simulation	Slope Determined from Experimental Measurement
Residence time	0.05 to 0.5 ms	0	0.004 ± 0.26 mV/ms
Channel length	1 to 8 mm	5 ± 4.6 mV/mm	0.5 ± 2.0 mV/mm
Channel width	0.25 to 1 mm	45 ± 46 mV/mm	18 ± 52 mV/mm
Channel depth	0.05 to 0.25 mm	−106 ± 25 mV/mm	−296 ± 90 mV/mm
Pore size	10 to 100 nm	1047 ± 155 mV/μm	1225 ± 400 mV/μm

Statistical analysis shows that channel length, channel width, and residence time have little or no effect on sensor response for both experiments and simulations. However, an increase in both pore size and a decrease in channel depth have the largest affect on response.

(slope close to zero) on sensor response. Conversely, channel depth has a large affect on sensor response in both simulation and experimental results. For example, both experimental and simulation results show a significant effect for decreasing channel depths. These results show that one important resistance is the mass transport of phosphonate diffusion perpendicular to the nanoporous membrane, and therefore depth of the microchannel is an important factor in sensor design.

Table 2 also shows that residence time has no affect on the response of the sensor. This trend is due to the saturation of the gas–liquid interface with phosphonate molecules. Most importantly, this trend shows that another rate determining step in phosphonate molecule transport occurs at the gas–liquid interface and the pore size of the nanoporous membrane is therefore extremely important. Accordingly, Table 2 shows that increasing pore size increases sensor response. This result shows that increasing the surface area of the gas–liquid interface has a large impact on sensor response.

From the simulation and experimental results, it was determined that the important resistances of the system are mass transport of phosphonate diffusion perpendicular to the nanoporous membrane and phosphonate molecule transport across the gas–liquid interface. Therefore, a microreactor with a shallow channel depth and large (at least 50 nm) porous membranes provided the best sensor response. From Eq. 4, we calculate a Thiele number of 0.09 after geometric optimization. A Thiele number much less than 1 means that our system is under kinetic limitations and this result shows that our microreactor geometry is now optimized.

$$\phi = h\sqrt{\frac{k}{D_{ab}}} \tag{3}$$

The optimized geometry provides a microsensor that has the extremely low sensitivity of 10^9 phosphonate molecules and has a rapid response.

Figure 7 shows the sensitivity of the oxime sensor before and after geometric optimization for a liquid microchannel 0.25 mm wide, 0.050 mm deep, and 5 mm long. In this experiment, the liquid microchannel contains 10 mM oxime solution and 1 cm^3/min of gas containing analyte flows in the vapor microchannel and potential is recorded after 30 s. In our geometric optimization, the channel depth was decreased from 0.1 mm to 0.05 mm and the pore size was increased from 10 to 50 nm. The limit of detection is found where the signal to noise ratio is equal to 3. The shape of the optimized curve is due to the exponential relationship between cyanide ion concentration and potential.

Note that the geometric optimization of our microsensor design decreased our detection limit by two orders of magnitude from 10^{11} to 10^9 phosphonate molecules. It is also important to note that the response of the optimized sensor at all concentrations is larger than the response from our previous design. The decrease in the detection limit and increase in sensor response makes our optimized sensor applicable for use in real-world phosphonate detection (e.g., pesticide detection in foodstuffs).

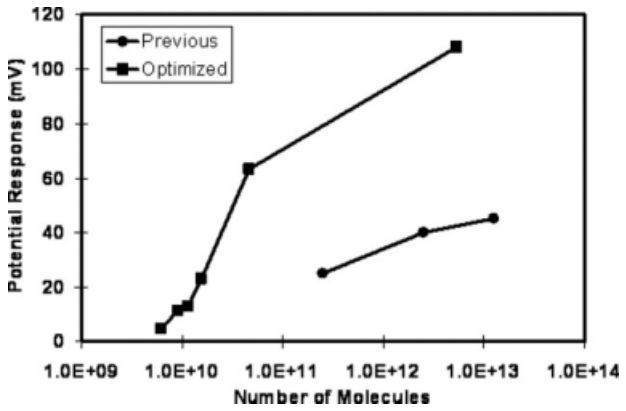

Figure 7. Sensitivity of oxime sensor before and after geometric optimization.

The circular points show that our previous sensor had a detection limit of more than 10^{11} molecules. After geometric optimization the detection limit of sensor was lowered two orders of magnitude to the order of 10^9 phosphonate molecules. Note that the response of our optimized sensor is larger than the response from our previous design.

Conclusions

In this study, a numerical simulation of our previously designed multiphase microreactor for use as a phosphonate sensor was created. The first generation phosphonate sensor showed promise initially; however, the sensitivity was insufficient for certain real-world applications. The COMSOL simulation was used to design a set of experimental conditions, to further optimize the microreactor. The experimental results were then compared with the numerical simulation to further understand the underlying transport phenomenon and optimize the senor geometry. Both experimental results and numerical simulation show that a decrease in channel depth and an increase in pore size allow for faster mass transport, faster sensor response, and lower detection limit.

The geometric optimization of the microsensor decreased our detection limit from 10^{11} to 10^{9} phosphonate molecules and also increased sensor response at all concentrations. The decrease in the detection limit and increase in sensor response makes our optimized sensor applicable for use in real-world phosphonate detection.

The results from this study show that future work should be done to optimize the reaction parameters, such as solvent, oxime concentration, and temperature. Also, the sensor should be tested with a range of interferents to access its selectivity. Using a mixture of buffer and aprotic solvents like ethanol will allow work with a higher oxime concentration while the solvent will act as a catalyst for the oxime reaction. The results from this study also show that fabrication of the microsensor should be done in silicon. For polycarbonate machining, 0.05 mm is the lower limit of channel depth. However, by moving the sensor into a silicon wafer, we can create smaller channels and may be able to further improve sensor response. Also, by creating a porous membrane with a silicon wafer, we can create a more hydrophobic membrane with a higher porosity. Optimizing the reaction parameters and fabricating the device in silicon will allow us to further improve sensor response and lower detection time.

Acknowledgments

This work was supported by the Defense Advanced Research Projects Agency (DARPA) under U.S. Air Force grant FA8650-04-1-7121. Any opinions, findings, and conclusions or recommendations expressed in this manuscript are those of the authors and do not necessarily reflect the views of the Defense Advanced Projects Research Agency, or the U.S. Air Force.

Literature Cited

1. Sun Y, Ong KY. *Detection Technologies for Chemical Warfare Agents and Toxic Vapors*. Boca Raton: CRC Press, 2005.
2. Eubanks LM, Dickerson TJ, Janda KD. Technological advancements for the detection of and protection against biological and chemical warfare agents. *Chem Soc Rev*. 2007;36:458–470.
3. Jain AV. Analysis of organophosphate and carbamate pesticides and anticholinesterase therapeutic agents. *Toxicol Organophosphate Carbamate Compd*. 2006;681–701.
4. Richardson SD. Water analysis: emerging contaminants and current issues. *Anal Chem*. 2007;79:4295–4323.
5. Ilwhan Oh, Monty CN, Masel RI. Electrochemical multiphase microreactor as fast, selective, and portable chemical sensor of trace toxic vapors. *IEEE Sensor J*. 2008;8:522–526.
6. Monty CN, Ilwhan Oh, Masel RI. Enzyme-based electrochemical multiphase microreactor for detection of trace toxic vapors. *IEEE Sensor J*. 2008;8:580–586.
7. Oh I, Masel RI. Electrochemical organophosphate sensor based on oxime chemistry. *Electrochem Solid State Lett*. 2007;10:J19–J22.
8. Welty W, Wilson R. *Fundamentals of Momentum, Heat, and Mass Transfer*, 4th ed. New York: Wiley, 2001.
9. Chung PMY, Kawaji M. The effect of channel diameter on adiabatic two-phase flow characteristics in microchannels. *Int J Multiphas Flow*. 2004;30:735–761.
10. Gunther A, Jensen KF. Multiphase microfluidics: from flow characteristics to chemical and materials synthesis. *Lab Chip*. 2006; 6: 1487–1503.
11. de Mas N, Gunther A, Kraus T, Schmidt MA, Jensen KF. Scaled-out multilayer gas-liquid microreactor with integrated velocimetry sensors. *Ind Eng Chem Res*. 2005;44:8997–9013.
12. Xu X, Wang X, Tang F, Zhou Z. The influencing factors of disposable acetylcholinesterase biosensor for in situ detection of organophosphorus pesticide. *Xiyou Jinshu Cailiao Yu Gongcheng*. 2006; 35:389–391.
13. Yen BKH, Gunther A, Schmidt MA, Jensen KF, Bawendi MG. A microfabricated gas-liquid segmented flow reactor for high-temperature synthesis: the case of CdSe quantum dots. *Angew Chem Int Ed*. 2005;44:5447–5451.
14. Kobayashi J, Mori Y, Okamoto K, Akiyama R, Ueno M, Kitamori T, Kobayashi S. A microfluidic device for conducting gas-liquid-solid hydrogenation reactions. *Science*. 2004;304:1305–1308.
15. Green AL, Saville B. The reaction of oximes with isopropyl methylphosphonofluoridate. *J Chem Soc*. 1956, 3887.
16. National Academies Press. *Review of the U.S. Army's Health Risk Assessments for Oral Exposure to Six Chemical-Warfare Agents*. National Academies Press, Washington DC, 1999.
17. Millington RJ. Gas diffusion in porous media. *Science*. 1959;130: 100–102.

Manuscript received Sep. 15, 2008, and revision received Mar. 16, 2009.